

An Efficient Light-Mediated Protocol for the Direct Amide Bond Formation via a Novel Carboxylic Acid Photoactivation Mode by Pyridine-CBr₄

Olga G. Mountanea,^[a, b] Danai Psathopoulou,^[a, b] Christiana Mantzourani,^[a, b]
Maroula G. Kokotou,^[c] E. Alexandros Routsis,^[a, b] Demeter Tzeli,^[d, e]
Christoforos G. Kokotos,^{*[a, b]} and George Kokotos^{*[a, b]}

To the memory of Leonidas Zervas, who together with Max Bergmann introduced the carbobenzyoxy group 90 years ago.

Abstract: The direct amide bond formation between a carboxylic acid and an amine still constitutes a challenging reaction for both academia and industry. We demonstrate herein that several pairs of amines (halogen bond acceptors) and organohalogen sources may be used for the photochemical amidation reaction under either UVA or sunlight irradiation. Our studies led to the identification of pyridine-CBr₄ as an efficient agent to perform amide synthesis under LED 370 nm irradiation, avoiding super-stoichiometric quantities. An extended substrate scope was demonstrated, show-

ing that the widely used amino and carboxyl protecting groups are compatible with this photochemical protocol, while a number of industrially interesting products and bioactive compounds were synthesized. Direct infusion-high resolution mass spectrometry studies suggest an unprecedented type of carboxylic acid activation mode upon irradiation, involving the generation of a symmetric anhydride, an active ester with pyridine *N*-oxide and a mixed anhydride with hypobromous acid.

Introduction

In the 21st century, the synthesis of the amide bond and the amino acid coupling still remains a challenging reaction. As highlighted in various review articles,^[1] the formation of the amide bond is one of the most frequently performed reactions, either in academia or in industry, possessing a 16% share of the total reactions used for the synthesis of new drugs.^[1c] In a 2006 survey, it was estimated that an amide bond was present in 2/3 of drugs candidates,^[1a] while our own search among the top 200 best-selling drugs in 2021^[2] revealed that at least 66 contained one amide bond.

So far, the method which possesses the lion's share in the amide bond formation and the peptide coupling involves the employment of coupling reagents.^[3] This widely used methodology requires the use of expensive reagents, often used in excess, in particular in solid phase peptide synthesis. In addition, some coupling reagents require demanding methods for their synthesis. As a consequence, during the last fifteen years considerable efforts have been devoted to the development of alternative methods, exploring non-classical routes.^[4] The development of catalytic methods are of high interest, however they have not flourished up to now, although interesting advances have been achieved.^[5] In any case, novel methods for amide bond formation are anticipated to have a high impact in industry, since large-scale amidations are very important in process chemistry.^[6]

In recent years, synthetic photochemistry and photocatalysis have captured the attention and imagination of organic

[a] O. G. Mountanea, D. Psathopoulou, Dr. C. Mantzourani, E. A. Routsis, Prof. Dr. C. G. Kokotos, Prof. Dr. G. Kokotos
Laboratory of Organic Chemistry, Department of Chemistry
National and Kapodistrian University of Athens
Panepistimiopolis, Athens 15771 (Greece)
E-mail: ckokotos@chem.uoa.gr
gkokotos@chem.uoa.gr

[b] O. G. Mountanea, D. Psathopoulou, Dr. C. Mantzourani, E. A. Routsis, Prof. Dr. C. G. Kokotos, Prof. Dr. G. Kokotos
Center of Excellence for Drug Design and Discovery
National and Kapodistrian University of Athens
Athens 15771 (Greece)

[c] Prof. Dr. M. G. Kokotou
Laboratory of Chemistry, Department of Food Science and Human Nutrition
Agricultural University of Athens
Iera Odos 75, Athens 11855 (Greece)

[d] Prof. Dr. D. Tzeli
Laboratory of Physical Chemistry, Department of Chemistry
National and Kapodistrian University of Athens
Panepistimiopolis Athens 15771 (Greece)

[e] Prof. Dr. D. Tzeli
Theoretical and Physical Chemistry Institute
National Hellenic Research Foundation
48 Vassileos Constantinou Ave., Athens 116 35 (Greece)

Supporting information for this article is available on the WWW under <https://doi.org/10.1002/chem.202300556>

© 2023 The Authors. Chemistry - A European Journal published by Wiley-VCH GmbH. This is an open access article under the terms of the Creative Commons Attribution Non-Commercial License, which permits use, distribution and reproduction in any medium, provided the original work is properly cited and is not used for commercial purposes.

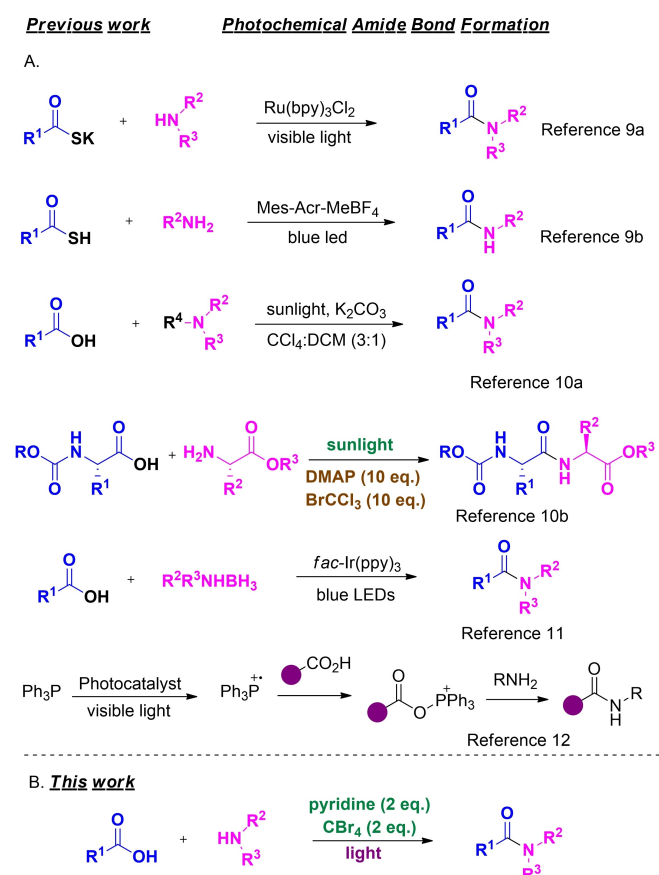
chemists, offering solutions to long-standing synthetic problems and the possibility to discover novel reactivities.^[7] The field of amide bond formation has not been unaffected by this revolutionary wave and several protocols for the visible light-mediated amide synthesis have been reported using various starting materials.^[8] In 2016, a remarkable visible-light-promoted photoredox catalytic methodology was demonstrated starting from ecofriendly potassium thioacids and amines, employing Ru(bpy)₃Cl₂ as the photocatalyst,^[9a] while some years later, a metal-free approach employing 9-mesityl-10-methylacridinium tetrafluoroborate (Mes-Acr-MeBF₄) for the coupling of thioacids and amines appeared (Scheme 1, A).^[9b] In 2017, Szpilman et al. reported the activation of amines under sunlight through a charge-transfer complex (CTC) and the subsequent coupling with acids, however the method was limited mainly in tertiary amines and aromatic acids (Scheme 1, A).^[10a] In 2021, Szpilman and coworkers presented a sunlight-mediated coupling of amino acids, which relies on the light activation of a 4-dimethylaminopyridine-bromotrichloromethane (DMAP-BrCCl₃) CTC to generate a novel coupling reagent in situ (Scheme 1, A).^[10b] At the same time, a photocatalytic deoxygenative amidation protocol employing amine-boranes and carboxylic acids was developed and used for the synthesis of a variety of functionalized amides and the late-stage functionalization of several pharmaceuticals (Scheme 1, A).^[11] Most recently, Zhao and co-workers have reported the synthesis of amides and

peptides through the generation of oxyphosphonium ions by photoredox/cobaloxime catalysis both in batch and continuous-flow (Scheme 1, A).^[12]

Working in the field of synthetic photochemistry^[13] and having developed protocols for the synthesis of amides starting from aldehydes,^[14] our attention has been captured by the method presented by Szpilman and coworkers,^[10b] which is based on the formation and photoactivation of a DMAP-BrCCl₃ complex. However, this method suffers from a serious drawback: the use of super-stoichiometric quantities of DMAP and BrCCl₃ (10 equivalents). The aim of our work was to study in detail the ability of selected amines to form halogen bonds (HBs) with various halogen bond donors, in an effort to define the factors that affect the generation of such complexes and their ability to be photoactivated, leading to coupling of carboxylic acids with amine components. UV-Vis and NMR studies, as well as computational calculations, were performed to understand the formation of halogen-bonded complexes (HBCs) and the subsequent successful carboxylic acid-amine coupling. We demonstrate herein that a combination of pyridine and carbon tetrabromide leads to successful coupling reactions of carboxylic acids with amine components, including amino acids, under UVA light irradiation, overcoming the drawback of super-stoichiometric quantities (Scheme 1, B). High resolution mass spectrometry (HRMS)-guided mechanistic studies of this new protocol unraveled an unprecedented activation mode of the carboxylic acid, involving the generation of a symmetric anhydride, an active ester of the carboxylic acid with pyridine *N*-oxide and a mixed anhydride between the carboxylic acid and hypobromous acid, as the active intermediates. The method has a wide substrate scope and can be applied in the synthesis of industrially relevant and bioactive compounds.

Results and Discussion

Although the formation of HBCs and their characterization as CTCs have been reported since the 1950s,^[15] only during the last 15 years such complexes have been recognized as efficient species to initiate and perform organic reactions, including organocatalytic or photocatalytic reactions.^[16] The photochemical amino acid coupling protocol published by Szpilman, Eichen et al. in 2021,^[10b] is based on the generation of a DMAP-BrCCl₃ complex, which upon sunlight activation leads to a successful coupling reaction. We envisaged that various couples of amines and halomethanes or halogen-containing compounds may form HBCs and subsequently such complexes may be activated by UVA or sunlight to mediate amidation reactions. Initially, we studied the potential formation of HBCs between the amines DMAP, *N,N*-dimethylaniline (DMA) or pyridine (as HB acceptors) and the halomethanes BrCCl₃, CBr₄, CCl₄, CH₂Br₂, or the bromine sources *N*-bromosuccinimide (NBS) and BrCH₂CN (as HB donors), in various solvents. DMAP, used by Szpilman et al.,^[10b] contains two distinct nitrogen atoms able to be involved in halogen bonding. DMA and pyridine were selected in order to understand how each one of the distinct nitrogen



Scheme 1. Literature methods for the amide bond formation and this work.

nitrogen) behaves in halogen bonding. For each pair of amine and halogen source, we recorded the UV-Vis spectra of the HB acceptor and the HB donor, each one alone, and of mixtures of HB acceptor and HB donor in 5.5:1 and 5.5:5 mole ratios in various solvents (Figures S2–S13 in Supporting Information).^[17] The UV-Vis spectra for the twelve pairs in acetonitrile (ACN), 1,2-dichloroethane (DCE), ethyl acetate (EtOAc) or acetone are shown in the Supporting Information (Figures S2–S13).^[17] Fig-

ure 1 summarizes the UV-Vis spectra for six pairs recorded in ACN.

In all studied solvents, the addition of BrCCl_3 into a solution of DMAP caused a red shift, which was clearly enhanced going from 5.5:1 to 5.5:5 mole ratio (Figure S2). This is in accordance with the observation of Szpilman et al. for UV-Vis spectra recorded in DCE.^[10b] The greatest shift was observed in ACN (Figure 1, A), thus ACN seems to be the most appropriate solvent for the HBC formation. A similar red shift was also

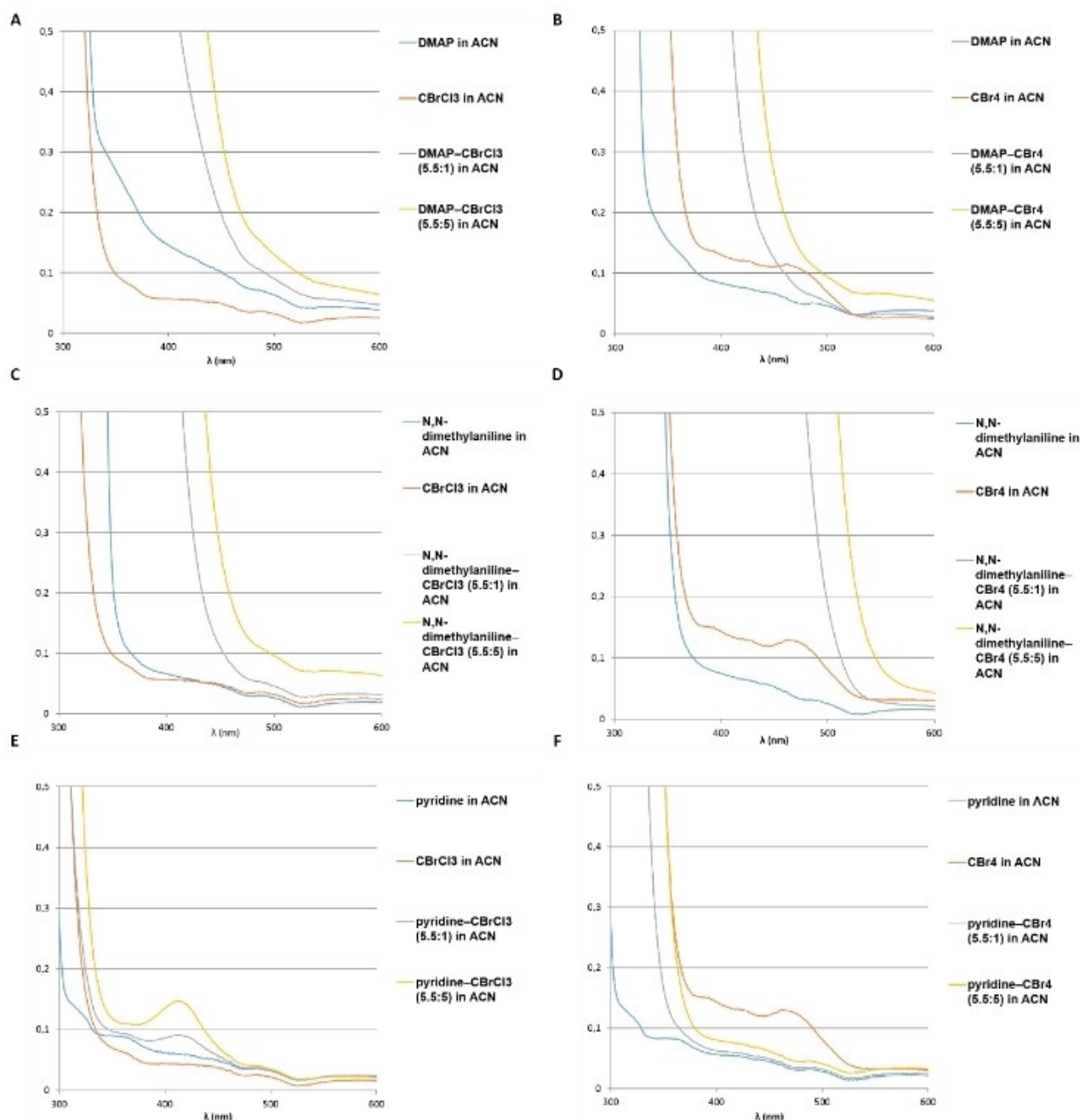


Figure 1. UV-Vis absorbance in acetonitrile (5 mL) of A. DMAP (5.5 mmol), BrCCl_3 (5 mmol), DMAP- BrCCl_3 (5.5 mmol:1 mmol) and DMAP- BrCCl_3 (5.5 mmol:5 mmol), B. DMAP (5.5 mmol), CBr_4 (5 mmol), DMAP- CBr_4 (5.5 mmol:1 mmol) and DMAP- CBr_4 (5.5 mmol:5 mmol), C. DMA (5.5 mmol), BrCCl_3 (5 mmol), DMA- BrCCl_3 (5.5 mmol:1 mmol) and DMA- BrCCl_3 (5.5 mmol:5 mmol), D. DMA (5.5 mmol), CBr_4 (5 mmol), DMA- CBr_4 (5.5 mmol:1 mmol) and DMA- CBr_4 (5.5 mmol:5 mmol), E. pyridine (5.5 mmol), BrCCl_3 (5 mmol), pyridine- BrCCl_3 (5.5 mmol:1 mmol) and pyridine- BrCCl_3 (5.5 mmol:5 mmol), F. pyridine (5.5 mmol), CBr_4 (5 mmol), pyridine- CBr_4 (5.5 mmol:1 mmol) and pyridine- CBr_4 (5.5 mmol:5 mmol).

observed in the case of DMAP-CBr₄ (Figure 1, B), while for the DMAP-CCl₄ or DMAP-CH₂Br₂ pairs, such a red shift was minimal (Figure S4 and S5).^[17] In the case of DMA, the addition of either BrCCl₃ or CBr₄ in ACN caused an enormous red shift, which was clearly enhanced going from 5.5:1 to 5.5:5 mole ratio (Figure 1, C and D), while the addition of CCl₄ caused a considerably lower shift and no shift was observed upon addition of CH₂Br₂ (Figure S8 and S9).^[17] For pyridine in ACN, a small shift was observed upon addition of either BrCCl₃ (Figure 1, E) or CCl₄ (Figure S12)^[17] in 5.5:5 mole ratio, while for CBr₄ such a shift was vague (Figure 1, F) and no shift was observed upon addition of CH₂Br₂ (Figure S13).^[17]

Table 1. ¹³C NMR (100 MHz, CDCl₃) shifts of halomethane carbon upon mixing with HB acceptors.^[17]

Entry	Amine-Halomethane	δ _c [ppm] before mix	δ _c [ppm] after mix	Δ [ppm]
1	DMAP + BrCCl ₃	67.58	67.34	0.24
2	DMAP + CBr ₄	-29.61	-28.66	0.95
3	DMAP + CCl ₄	96.15	95.86	0.29
4	DMAP + CH ₂ Br ₂	18.95	18.88	0.07
5	DMA + BrCCl ₃	67.58	67.55	0.03
6	DMA + CBr ₄	-29.61	-29.24	0.37
7	DMA + CCl ₄	96.15	96.10	0.05
8	DMA + CH ₂ Br ₂	18.97	18.93	0.04
9	Pyridine + BrCCl ₃	67.58	67.41	0.17
10	Pyridine + CBr ₄	-29.60	-29.17	0.43
11	Pyridine + CCl ₄	96.15	95.97	0.18
12	Pyridine + CH ₂ Br ₂	18.95	18.89	0.06

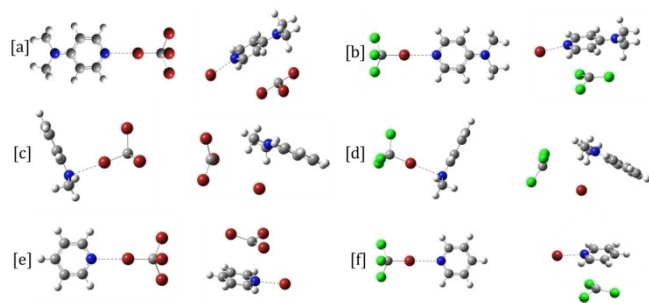


Figure 2. Calculated structures of the halogen-bonded complexes (left) and their first excited triplet states (right) at the wB97X-D/def2TZVP method; a. DMAP-CBr₄, b. DMAP-BrCCl₃, c. DMA-CBr₄, d. DMA-BrCCl₃, e. Pyridine-CBr₄, f. Pyridine-BrCCl₃.

Halogen bonding propensity in solution is usually predicted by computational approaches and only very recently Raman spectroscopy has found application for direct observation.^[18] In the present study, to further understand the interactions between the various HB donors and acceptors, we recorded ¹³C NMR spectra of a solution of each halomethane alone and the corresponding mixture of halomethane-amine and the shifts observed for halomethane carbon atom are summarized in Table 1. When DMAP was mixed with BrCCl₃ or CBr₄ or CCl₄ or CH₂Br₂, the highest shift was recorded for CBr₄ (0.95 ppm, entry 2, Table 1). The shifts observed for CCl₄ (0.29 ppm) or BrCCl₃ (0.24 ppm) were similar (entries 1 and 3, Table 1), while the shift for CH₂Br₂ was negligible (0.07 ppm, entry 4, Table 1). For mixtures consisting of DMA and halomethane, a shift was observed only in the case of CBr₄ (0.37 ppm, entry 6, Table 1). For pyridine, again the highest shift was recorded in the case of CBr₄ (0.43 ppm, entry 10, Table 1). Small shifts for CCl₄ or BrCCl₃ were also observed, while the shift for CH₂Br₂ was negligible. These results suggest that ¹³C NMR spectroscopy enables the identification of interactions, suggesting the formation of halogen bonding. For all studied HB acceptors (DMAP, DMA, pyridine), the most notable shifts were observed in the case of CBr₄ as the HB donor.

To further explore the generation of HBCs and their properties, DFT studies (wB97X-D^[19]/def2TZVP^[20]) in ACN solvent were carried out. The ground state (*S*₀, singlet) and the lowest calculated in energy triplet state (*T*₁) of the HBCs DMAP-CBr₄, DMAP-BrCCl₃, DMA-CBr₄, DMA-BrCCl₃, pyridine-CBr₄ and pyridine-BrCCl₃ are depicted in Figure 2 and selected geometries are summarized in Table 2. In the ground states, a weak Br⋯N bond is formed and the C–Br⋯N angle is almost linear (see, Table 2). For both DMAP and pyridine, the Br⋯N bond is about 2.8 Å, while for DMA is about 2.9 Å, due to stereochemical restrictions resulting from the methyl groups. Additionally, when its N atom interacts with Br, it does not have a planar geometry, and the CCNC dihedral angle is 145.8 degrees. On the contrary, the Br⋯N bond does not affect the geometries of the N atoms in DMAP and in pyridine. In the lowest in energy triplet states (*T*₁), the C–Br bond has been cleaved and the [•]CBr₃ and [•]CCl₃ radicals are formed. In the case of DMAP or pyridine, the Br atom is connected to the nitrogen of the pyridine ring, and the Br⋯N bond becomes shorter by 0.3 Å and 0.35 Å, respectively. On the contrary, in the case of DMA, the N⋯Br bond is elongated by 0.6 Å and the CCNC dihedral angle from

Table 2. Calculated C–Br and Br⋯N bond distances (Å), C–Br⋯N angles (degrees), and CCNC dihedral angles (degrees) for all XB donors and halogen bonded complexes in ACN solvent at the wB97X-D/def2TZVP level of theory.

HB Donor & HB complex	C–Br ^[a]	C–Br⋯N ^[a]	C–Br⋯N angle ^[a]	CCNC angle ^[a]	C–Br⋯N ^[b]	CCNC angle ^[b]
CBr ₄	1.938					
DMAP-CBr ₄	1.945	2.773	179.99		2.470	
DMA-CBr ₄	1.941	2.927	178.69	145.8	3.550	171.1
pyridine-CBr ₄	1.943	2.824	179.91		2.482	
BrCCl ₃	1.944					
DMAP-BrCCl ₃	1.949	2.781	179.94		2.470	
DMA-BrCCl ₃	1.946	2.940	179.19	145.7	3.561	171.5
pyridine-BrCCl ₃	1.947	2.830	179.88		2.483	

[a] Ground state (*S*₀). [b] First excited triplet state (*T*₁).

145.8 degrees in the S_0 state becomes almost planar at 171.1 degrees in the T_1 state. Note that changes in the dihedral geometry of the N atom are associated with the properties of compounds.^[21]

The strongest binding energy (ΔE_{bind}) is observed for the DMA- CBr_4 pair at -4.59 kcal/mol, even though the N atom of DMA is not planar, while the weakest one is found for the pyridine- BrCCl_3 at -3.78 kcal/mol (Table 3). DMA forms the most stable donor-acceptor pairs, and it presents the lowest adiabatic $S_0 \rightarrow T_1$ excitation energy, that is, 24.9 kcal/mol (DMA- CBr_4) (Table 4). This means that the triplet state for DMA is thermodynamically the most stable, meaning that it is the least reactive. On the contrary, pyridine forms the least stable donor-acceptor pairs, and it presents the highest adiabatic $S_0 \rightarrow T_1$ excitation energy, 38% than DMA- CBr_4 (Table 4). Thus, we can conclude that pyridine complexes more easily react towards the next steps of the photochemical reaction than the other complexes. All the above spectroscopic and computational studies show that indeed DMAP, DMA and pyridine may form halogen bonds with CBr_4 and BrCCl_3 , although the properties and the strength of such a bond seem to vary.

Then, we studied the photochemical coupling of Z-L-phenylalanine (Z-Phe-OH, 1) to ethyl glycinate (H-Gly-OEt, 2), using DMAP or DMA and various HB donors, under light irradiation. Ten equivalents of DMAP and HB donors (BrCCl_3 , CBr_4 , CCl_4 , CH_2Br_2 , NBS or BrCH_2CN) and two equivalents of the amine component were used in all cases. The results are summarized in Table 5 (full studies are presented in Tables S1 and S2).^[17] After a reaction time of 6 h, the highest yield was achieved under LED irradiation at 370 nm in ACN (75% yield, entry 3 vs. 1, Table 5), while under sunlight, 67% yield was recorded (entry 4, Table 5). It should be noticed that using 2 equivalents of DMAP and BrCCl_3 , the product was obtained in only 16% yield (entry 2, Table 5). Both CBr_4 and CCl_4 proved less efficient agents, leading to 71% and 65% yield (entries 5 and 7, Table 5) of isolated product under LED 370 nm, while under sunlight, the yield using CBr_4 was 59% (entry 6, Table 5). The

Table 3. Calculated theoretical binding energies (ΔE_{bind} in kcal mol⁻¹) of all halogen-bonded complexes in ACN solvent at the wB97X-D/def2TZVP methodology.

HB Acceptors	HB Donors	
	CBr_4	BrCCl_3
DMAP	-4.43	-4.30
DMA	-4.59	-4.37
Pyridine	-3.89	-3.78

Table 4. Calculated vertical (ΔE_v) and adiabatic (ΔE_a) singlet-triplet excitation energy in kcal mol⁻¹ of all halogen-bonded complexes in ACN solvent at the wB97X-D/def2TZVP level of theory.

Halogen-bonded complex	ΔE_v	ΔE_a
DMAP- CBr_4	87.3	31.2
DMAP- BrCCl_3	87.3	33.1
DMA- CBr_4	84.2	24.9
DMA- BrCCl_3	84.3	26.1
pyridine- CBr_4	92.3	34.2
pyridine- BrCCl_3	92.3	35.7

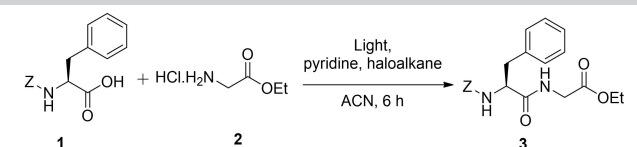
Table 5. Photochemical coupling of Z-L-Phe-OH (1) to HCl-H-Gly-OEt (2) using DMAP or DMA and various HB donors.^[a]

Entry	Haloalkane	HB acceptor	Light	Yield [%] ^[b]
1 ^[c]	BrCCl_3	DMAP	370 nm	69
2 ^[c,d]	BrCCl_3	DMAP	370 nm	16
3	BrCCl_3	DMAP	370 nm	75
4	BrCCl_3	DMAP	sunlight	67
5	CBr_4	DMAP	370 nm	71
6	CBr_4	DMAP	sunlight	59
7	CCl_4	DMAP	370 nm	65
8	CH_2Br_2	DMAP	370 nm	10
9	NBS	DMAP	370 nm	11
10	BrCH_2CN	DMAP	370 nm	1
11 ^[c]	BrCCl_3	DMA	370 nm	50
12	BrCCl_3	DMA	370 nm	77
13	BrCCl_3	DMA	sunlight	69
14	CBr_4	DMA	370 nm	62
15	CBr_4	DMA	sunlight	48
16 ^[e]	CBr_4	DMA	370 nm	15
17	CCl_4	DMA	370 nm	42
18	CH_2Br_2	DMA	370 nm	0
19	NBS	DMA	370 nm	5
20	BrCH_2CN	DMA	370 nm	0

[a] Reaction conditions: 1 (0.28 mmol), 2 (0.56 mmol), DMAP or DMA (2.80 mmol), haloalkane (2.80 mmol), ACN (4.25 mL), light irradiation at r.t.
 [b] Yield of 3 after isolation by column chromatography. [c] DCE (4.25 mL) was used instead of ACN. [d] 2 equivalents of DMAP and BrCCl_3 were employed. [e] 2 equivalents of DMA and CBr_4 were employed.

result for CBr_4 is in contrast to that reported by Szpilman et al.,^[10b] reporting no formation of the desired amide product using DMAP- CBr_4 under sunlight. In the case of CCl_4 , it is in accordance with Szpilman et al.,^[10b] who reported that under sunlight, CCl_4 had to be used as a co-solvent to reach a satisfactory yield, requiring extended reaction time and increased excess of the amino component. The other bromine sources used (CH_2Br_2 , NBS and BrCH_2CN) led to very low yields (entries 8–10, Table 5). The results for the studies using DMA and various HB donors are also presented in Table 5. Similar trends to DMAP were observed after 6 h (entries 11–13, Table 5), and the highest yield of isolated product was 77% (entry 12, Table 5). Lower yields were observed for DMA- CBr_4 (entries 14–16, Table 5), while again a dramatic drop of the yield was observed, when the equivalents of DMA and HB donor were reduced to 2 (entry 16, Table 5). The product was isolated in lower yields when DMA- CCl_4 was employed (entry 17, Table 5), while none of CH_2Br_2 , NBS and BrCH_2CN practically led to product (entries 18–20, Table 5).

Next, the combination of pyridine with various HB donors was studied (Table 6 and Table S3). First, ten equivalents of pyridine and BrCCl_3 or CBr_4 or CCl_4 and two equivalents of the amine component were used (entries 1–4, Table 6). The coupling product was isolated in high yield using CBr_4 (83%, entry 3, Table 6) after 6 h of LED irradiation at 370 nm, while lower yield was found using BrCCl_3 and practically no reaction was observed using CCl_4 under the same conditions (entries 1

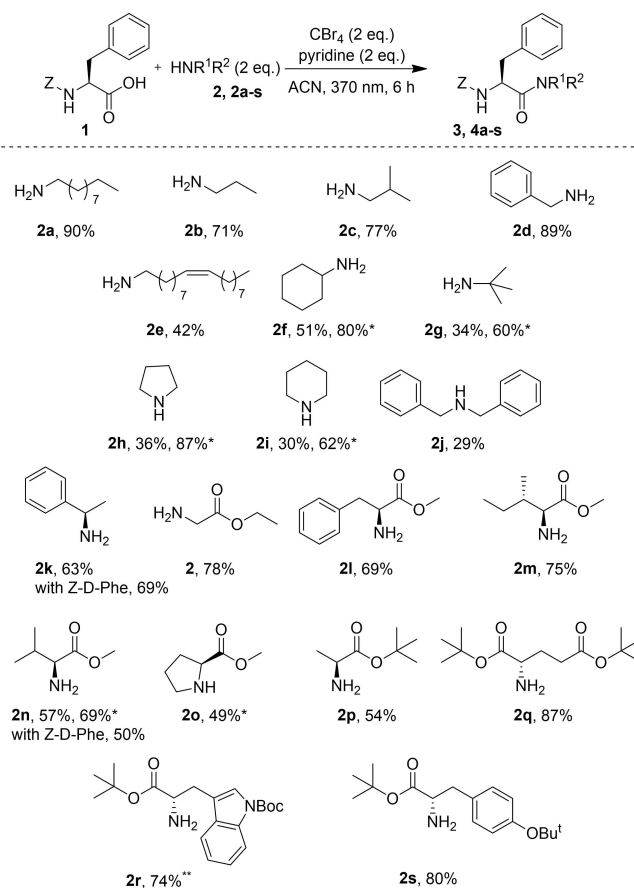
Table 6. Optimization of the photochemical coupling of Z-L-Phe-OH (1) to HCl.Gly-OEt (2) using pyridine and various haloalkanes.^[a]


Entry	Haloalkane [equiv.]	Pyridine [equiv.]	Light	Yield [%] ^[b]
1	BrCCl ₃ , 10	10	370 nm	47
2	CCl ₄ , 10	10	370 nm	1
3	CBr ₄ , 10	10	370 nm	83
4	CBr ₄ , 10	10	sunlight	25
5	CBr ₄ , 2	2	370 nm	78
6	CBr ₄ , 2	2	dark	0
7	CBr ₄ , 2	2	390 nm	77
8	CH ₂ Br ₂ , 10	10	370 nm	1
9 ^[c]	CBr ₄ , 2	2	370 nm	71
10 ^[d]	CBr ₄ , 2	2	370 nm	54
11	CBr ₄ , 1	2	370 nm	59

[a] Reaction conditions: 1 (0.28 mmol), 2 (0.56 mmol), pyridine, haloalkane, ACN (4.25 mL), light irradiation at r.t. [b] Yield of 3 after isolation by column chromatography. [c] 1.5 equivalent of 2. [d] 1 equivalent of 2.

and 2, Table 6). Sunlight was proven ineffective, leading to low yield (entry 4, Table 6). Gratifyingly, 80% yield was achieved when the equivalents of pyridine and CBr₄ were reduced to 5 (Table S3).^[17] The yield remained high (78%), even when 2 equivalents of pyridine and CBr₄ were used (entry 5, Table 6), indicating that super-stoichiometric quantities of amine-organohalogen components may be overcome. Under dark, no product was obtained (entry 6, Table 6), while irradiation at higher wavelength resulted in slightly lower yield (entry 7, Table 6). As in the case of DMAP and DMA, the use of CH₂Br₂ did not lead to product (entry 8, Table 6). Efforts to modify the ratio of pyridine, CBr₄ and amine component led to lower yields (entries 9–11, Table 6).

Our detailed study of various HB donors and acceptors pairs revealed that indeed various pairs enable the amidation reaction. However, pyridine-CBr₄ stands out as a very efficient combination for an amidation reaction, under LED 370 nm irradiation in ACN, bypassing the need for super-stoichiometric quantities and leading to the highest yield of the desired product. To explore the substrate scope of this new photochemical protocol, we studied the coupling of Z-L-phenylalanine (1) to various amine components and the results are summarized in Scheme 2. Aliphatic saturated amines **2a–c**, as well as benzylamine (**2d**), coupled in high to excellent yields (71–90%). The product of coupling to oleyl amine (**2e**) was isolated in 42% yield, accompanied by addition products to the double bond, indicating that unsaturated compounds have limitations. Primary amines, such as **2f** and **2g**, on secondary or tertiary substituted carbon atoms, required a higher pyridine-CBr₄ ratio (5 equivalents) to reach 60–80% coupling yields. Secondary amines, such as pyrrolidine (**2h**) and piperidine (**2i**), afforded the coupling products in high to excellent yields, but a higher pyridine-CBr₄ ratio was required. Dibenzylamine (**2j**) led to lower yield. Chiral amine **2k** coupled well with both Z-L-Phe-OH or Z-D-Phe-OH. Coupling of a variety of C-

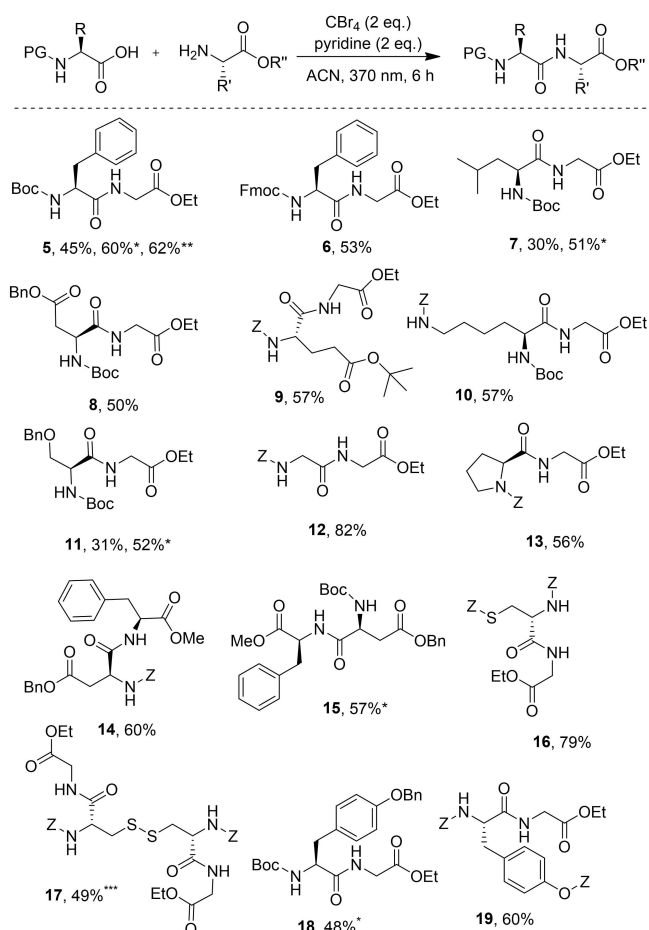


Scheme 2. Light-mediated coupling of Z-Phe-OH to various amine components using pyridine-CBr₄: Acid (0.28 mmol), amine (0.56 mmol), pyridine (0.56 mmol, 0.05 mL) and CBr₄ (0.56 mmol, 186 mg) in ACN (4.25 mL). * 5 eq. pyridine, 5 eq. CBr₄. ** 3 eq. pyridine.

protected amino acids **2** and **2l–s** (methyl, ethyl or *tert*-butyl esters) provided the products in moderate to excellent yields (54–87%). In the case of the sterically hindered valine (**2n**) or the secondary amine proline (**2o**), a higher pyridine-CBr₄ ratio may increase the yield. HPLC analysis of the coupling products of Z-L-Phe-OH or Z-D-Phe-OH to α -(*R*)-methyl benzylamine or methyl L-valinate, using a chiral column, showed that the light-mediated coupling protocol is free of epimerization.^[17]

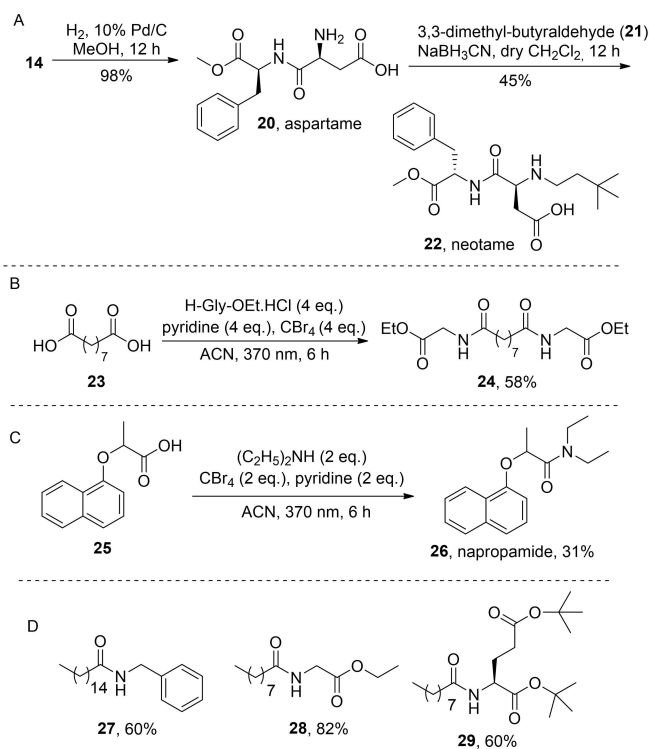
Then, we focused on the synthesis of dipeptides and the results are summarized in Scheme 3. Various commonly used in peptide synthesis amino protecting groups (benzyloxycarbonyl, Z, *tert*-butoxycarbonyl, Boc, and fluorenylmethyloxycarbonyl, Fmoc) and carboxy protecting groups (methyl, ethyl, benzyl, *tert*-butyl) were found compatible with this photochemical protocol, affording the dipeptides in yields ranging from 48–82%. In general, the yield of the coupling reaction may increase, if the pyridine-CBr₄ ratio is increased.

Our photochemical protocol was further applied to the synthesis of industrially interesting products (Scheme 4). Aspartame (**20**) and neotame (**22**) are synthetic sweeteners, which are widely used in food industry, for example in refreshments, yogurts, lactic beverages, desserts, etc. and are produced in thousand tons annually.^[22] Photochemical coupling of Z-



Scheme 3. Light-mediated synthesis of dipeptides using pyridine- CBr_4 : Acid (0.28 mmol), amine (0.56 mmol), pyridine (0.56 mmol, 0.05 mL) and CBr_4 (0.56 mmol, 186 mg) in ACN (4.25 mL). * 3 equiv. pyridine. ** 4 equiv. pyridine. *** 4 equiv. pyridine, 4 equiv. amine, 4 equiv. CBr_4 .

Asp(OBn)-OH to H-Phe-OMe provided dipeptide **14** in 60% yield (Scheme 3), which after hydrogenation afforded aspartame **20** in 98% yield and subsequently neotame **22** after reductive amination with 3,3-dimethylbutyraldehyde (**21**) (Scheme 4, A). Azeloyl diglycinate, in the form of its potassium salt, finds use in cosmetics, exhibiting sebostatic and whitening action and offering a moisturizing effect, due to glycine.^[23] Azelaic acid **23** was coupled to H-Gly-OEt, affording **24** in 58% yield (Scheme 4, B). Napropamide belongs to the amide herbicide family, and in its racemic form is widely used for pre-emergence control of annual grasses and broad-leaved weeds in many crops.^[24] Coupling of **25** to diethylamine produced **26** in low yield (Scheme 4, C). Macamides are a unique class of long chain fatty acid *N*-benzylamides, constituting the major bioactive compounds of Maca, exhibiting fertility-enhancing, neuroprotective and neuro-modulatory, anti-fatigue and anti-osteoporosis activities.^[25] Fatty acid acyls constitute an important family of endogenous signaling molecules that may regulate pain and inflammation.^[26] Photochemical coupling of palmitic acid and pelargonic acid to benzylamine and amino



Scheme 4. Applications of the light-mediated pyridine- CBr_4 protocol for the synthesis of industrially interesting compounds and bioactive compounds: A. Artificial sweeteners aspartame and neotame, B. Azeloyl diglycinate, C. Napropamide, D. Macamide and fatty acid acyls.

acid esters, respectively, afforded palmitoyl benzylamide (**27**) and conjugates **28** and **29** in 60%–82% yields (Scheme 4, D).

The mechanism of the UVA-mediated coupling using pyridine- CBr_4 was studied by direct infusion-high resolution mass spectrometry (DI-HRMS). DI-HRMS finds interesting applications in non-targeted metabolomics as an alternative approach to chromatography-MS-based techniques.^[27] We have successfully employed DI-HRMS for the elucidation of organic reaction mechanisms,^[13d,28] because it offers a rapid and simplified approach, avoiding time-consuming chromatography and possible decomposition of sensitive to solvents analytes. Selected data of the HRMS analysis for the coupling of Z-Phe-OH to H-Gly-OEt utilizing pyridine- CBr_4 under LED 370 nm irradiation are depicted in Figure 3. Details on the mechanistic studies by DI-HRMS are described in the Supporting Information.^[17]

We began the DI-HRMS mechanistic investigation, studying the interaction of pyridine with CBr_4 after irradiation at 370 nm. Upon such irradiation, intermediate I (Scheme 5) was generated, whose cationic species was clearly observed by HRMS (Figure 3, B).^[17] In addition, an ion corresponding to pyridine *N*-oxide II was formed (Figure 3, B). When a mixture of Z-Phe-OH, pyridine and CBr_4 was irradiated at 370 nm, intermediates I and II were also observed. However, monitoring the full scan spectrum of the reaction mixture, our attention was captured by an ion observed at m/z 603.2091 (Figure 3, A). This ion was recorded from the beginning of the reaction (30 min) and was

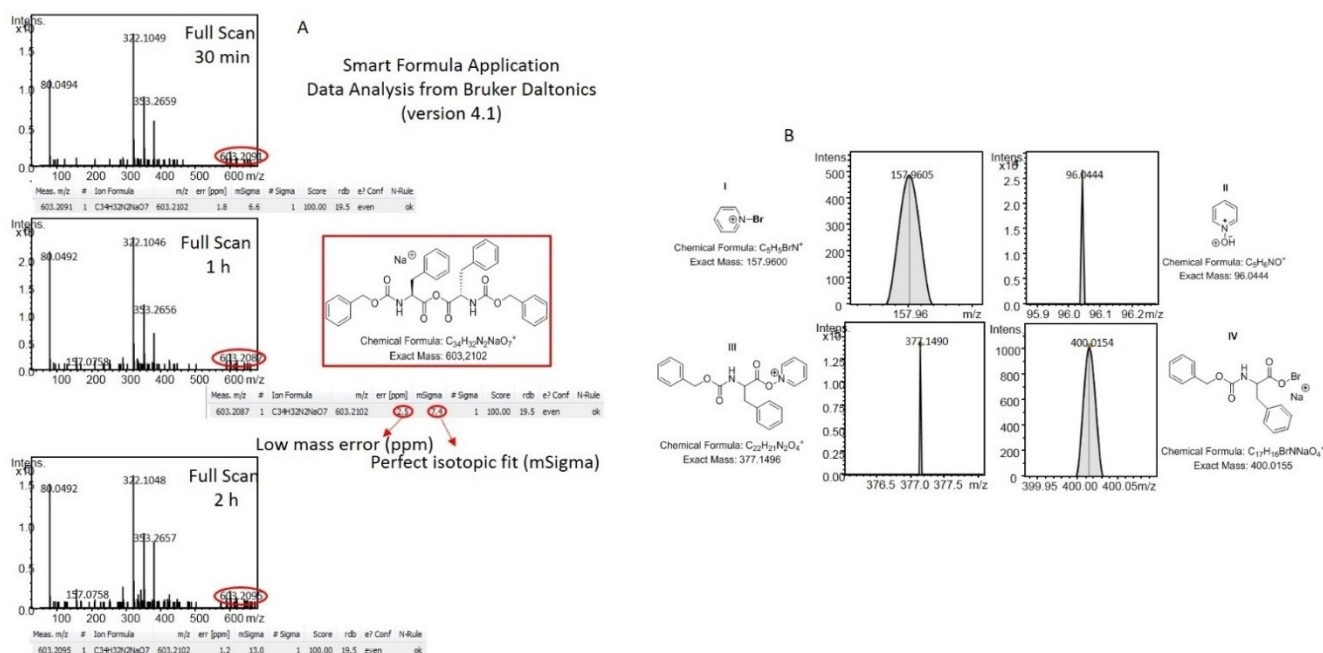
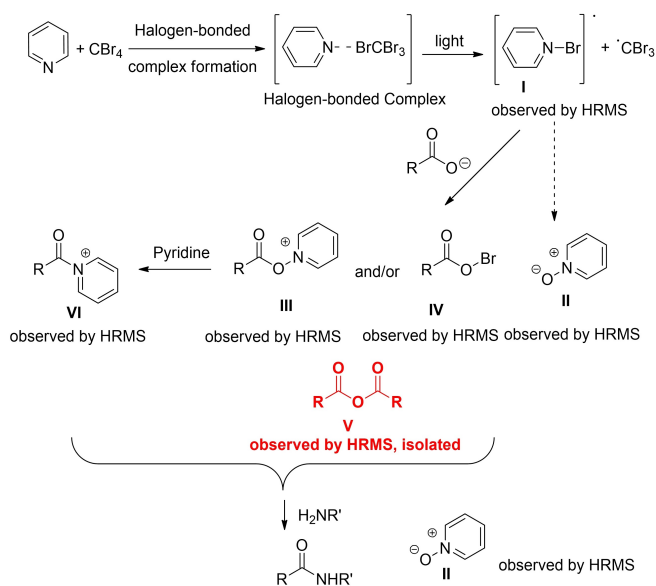


Figure 3. A. Monitoring of activation of Z–Phe–OH by pyridine and CBr_4 under LED 370 nm irradiation. Full scan HRMS spectra verifying the generation of symmetric anhydride (m/z 603.2102), B. Selected extracted ion chromatograms indicating the formation of various intermediates during the photochemical coupling of Z–Phe–OEt to H–Gly–OEt.



Scheme 5. HRMS-guided proposed mechanism for the photochemical coupling of carboxylic acid $RCOOH$ to amine $R'NH_2$ using pyridine- CBr_4 .

present during the entire time course of the study (up to 3 h). Using Smart Formula application of Data Analysis from Bruker Daltonics (version 4.1), this measured exact mass was found to correspond to $C_{34}H_{32}N_2NaO_7^+$ (excellent mass error and isotopic fit) (Figure 3, A), which may be attributed to the formation of the symmetric anhydride of Z–Phe–OH (intermediate V). To explain the generation of such an intermediate, we searched for possible activated forms of Z–Phe–OH. Indeed, ions which may

be attributed to the formation of two activated intermediates of Z–Phe–OH were detected. The most intense peak may correspond to the acyloxy pyridinium intermediate III (Figure 3, B), which may play a role as the active ester of Z–Phe–OH with pyridine *N*-oxide. In addition, an ion that may correspond to a mixed anhydride of Z–Phe–OH with hypobromous acid (intermediate IV) was observed (Figure 3, B). Both of them may generate the symmetric anhydride V upon their reaction with the carboxylate anion. In addition, a low abundance ion, which may be attributed to an acyl pyridinium ion of Z–Phe–OH (intermediate VI) was recorded.^[17] When a mixture of Z–Phe–OH, pyridine and CBr_4 was stirred under dark, none of the ions corresponding to intermediates III, IV and V were observed. Next, we monitored the mixture of the coupling reaction (Z–Phe–OH, H–Gly–OEt, pyridine, CBr_4) upon irradiation at 370 nm. Ions corresponding to the symmetric anhydride V, as well as all the activated intermediates of Z–Phe–OH were recorded,^[17] providing clear experimental evidence for a multiple activation mode of the carboxylic acid component. Our attempts to isolate the symmetric anhydride of Z–Phe–OH from the reaction mixture failed. However, we succeeded to isolate palmitic anhydride, when a mixture of palmitic acid, pyridine and CBr_4 was irradiated at 370 nm for 3 h.^[17]

Taking all the above data into account, a plausible mechanism may be proposed, as shown in Scheme 5. Initially, halogen bonding between pyridine and CBr_4 occurs. After irradiation of the coupling reaction mixture, intermediate I is formed. Then, various activated carboxylic acid intermediates are generated (symmetric anhydride V, active ester with pyridine oxide III, mixed anhydride with hypobromous acid IV),

which may lead to the coupling product after the successful nucleophilic attack of the amine component. The symmetric anhydrides are well known activated intermediates for use in amide and peptide coupling,^[29] and this may be the major pathway in the present photochemical protocol, leading to coupling product. Based on the high abundance of the ion corresponding to the acyloxy pyridinium intermediate **III**, we suggest that this intermediate may also play a key-role. 4-(Dimethylamino)pyridine *N*-oxide (DMAPO) has been described as an effective catalyst in peptide coupling reactions.^[30a] In addition, such an activated derivative has been synthesized from DMAPO and cinnamoyl chloride and successfully used for coupling with an amine.^[30b] In our photochemical protocol, we propose that the reactive acyloxy pyridinium intermediate is generated *in situ* as a result of the pyridine-CBr₄ mixture irradiation. To our knowledge, this is the first time such an activated intermediate based on pyridine *N*-oxide is observed and proposed as an effective intermediate for the amide bond formation. In parallel, a mixed anhydride of Z-Phe-OH with hypobromous acid (intermediate **IV**) may lead to the coupling product after attack of the amine component. Mixed anhydrides of carboxylic acids with inorganic acids have been studied for the coupling reaction at older times,^[31] but at the end mixed carbonic anhydrides have been extensively used in peptide synthesis. Again, to our knowledge this is the first time a mixed anhydride of a protected amino acid with hypobromous acid is proposed as effective intermediate for amidation reaction. Finally, the acyl pyridinium intermediate **VI** may be formed, leading to the final product after attack by the amine.

To sum up, careful monitoring and examination of the HRMS spectra suggested the generation of unprecedented carboxylate intermediates. The symmetric anhydride of palmitic acid was isolated, confirming that this intermediate plays a key-role in this light-mediated protocol.^[17] Thus, a thorough study involving UV-Vis, NMR, DFT calculations, DI-HRMS and experimental data revealed a new activation process for the coupling of carboxylic acids with amines, employing a low reagent ratio of pyridine-CBr₄ (2 equivalents). The present protocol significantly differs from the procedure introduced by Szpilman et al.,^[10b] not only in the reaction mechanism, but also in reagent stoichiometry. Szpilman et al. demonstrated that DMAP-BrCCl₃ is a unique couple of CTC in DCE that when used in super-stoichiometric amounts (10 equivalents) is able to afford amide bond formation under sunlight, while the authors postulated the generation of a hemiaminal ester of carboxylic acid via iminium salt formation (distinctively different than the species presented in the present study) as the active intermediate that drives the reaction.^[10b] Herein, we demonstrate that various pairs of HB donors and acceptors can form HBCs that can promote the amide bond formation under 370 nm LED irradiation or sunlight. The use of pyridine-CBr₄ stands out and can overcome the necessity for super-stoichiometric amounts of reagents, working equally well when only two equivalents are employed. Extended spectroscopic and theoretical studies revealed the complicated nature of the reaction mechanism, which significantly differs in our protocol (different active

intermediates are involved) and this is possibly the reason that lowering the amount of the reagents is feasible.

Conclusion

In conclusion, the detailed study of several pairs of amines and organohalogen sources revealed that various pairs may be used for a photochemical amidation reaction under either UVA or sunlight. Inexpensive pyridine-CBr₄ was identified as an efficient agent to perform amide bond formation reactions under LED 370 nm irradiation, avoiding super-stoichiometric quantities. The widely used amino protecting groups (Z, Boc, Fmoc) and carboxy protecting groups (methyl, ethyl, benzyl, *tert*-butyl) are compatible with this photochemical protocol. Applications of the new photochemical protocol for the synthesis of industrially interesting products and bioactive compounds were demonstrated. DI-HRMS studies shed light on the mechanism of the reaction, suggesting the light-mediated formation of a symmetric anhydride, an active ester of the carboxylic acid with pyridine *N*-oxide and a mixed anhydride between the carboxylic acid and hypobromous acid as the reactive intermediates. Thus, a novel efficient and low-cost photochemical protocol for the amide bond formation is demonstrated, uncovering the possibility of novel activation mode of a carboxylic acid under photoactivation of the pyridine-CBr₄ mixture.

Experimental Section

In a 25 mL Schlenk tube equipped with a PTFE-coated stirring bar, the appropriate acid (0.28 mmol), the amine (0.56 mmol), pyridine (0.56 mmol, 0.05 mL) and CBr₄ (0.56 mmol, 186 mg) along with ACN (4.25 mL, HPLC grade) were added. The reaction mixture was stirred under light irradiation (Kessil lamps 370 nm) for 6 h. Then, the solvent was removed under vacuum and the crude reaction mixture was treated with aqueous citric acid 10% (10 mL), before it was extracted with CH₂Cl₂ (3 × 10 mL). The combined organic layers were washed with H₂O (10 mL), aqueous NaHCO₃ (10 mL) and brine (1 × 10 mL), dried over Na₂SO₄, filtered and concentrated under reduced pressure. The desired product was purified by column chromatography.

Acknowledgements

The research presented was carried out within the framework of a Stavros Niarchos Foundation grant to the National and Kapodistrian University of Athens (G.K.). The authors gratefully acknowledge the Hellenic Foundation for Research and Innovation (H.F.R.I.), since this research project was supported by the Hellenic Foundation for Research and Innovation (H.F.R.I.) under the "1st Call for H.F.R.I. Research Projects to support Faculty Members & Researchers and the Procurement of High-cost research equipment grant" (grant number 655) (C.G.K.). The research work was supported by the Hellenic Foundation for Research and Innovation (H.F.R.I.) under the H.F.R.I. PhD Fellowship grant (Fellowship Number: 1338) (O.G.M.).

Conflict of Interests

The authors declare no conflict of interest.

Data Availability Statement

The data that support the findings of this study are available in the Supporting Information of this article.

Keywords: amide bond formation · DFT calculations · halogen bonding · light-mediated chemistry · peptides

- [1] For selected reviews, see: a) J. S. Carey, D. Laffan, C. Thomson, M. T. Williams, *Org. Biomol. Chem.* **2006**, *4*, 2337–2347; b) S. D. Roughley, A. M. Jordan, *J. Med. Chem.* **2011**, *54*, 3451–3479; c) D. G. Brown, J. Boström, *J. Med. Chem.* **2016**, *59*, 4443–4458.
- [2] Top 200 Drugs, 2021. <https://njardarson.lab.arizona.edu/sites/njardarson.lab.arizona.edu/files/Top%20200%20Pharmaceuticals%202021%20V2.pdf> (accessed 2022–12–28).
- [3] For selected reviews, see: a) S.-Y. Han, Y.-A. Kim, *Tetrahedron* **2004**, *60*, 2447–2467; b) C. A. G. N. Montalbetti, V. Falque, *Tetrahedron* **2005**, *61*, 10827–10852; c) A. El-Faham, F. Albericio, *Chem. Rev.* **2011**, *111*, 6557–6602.
- [4] For selected reviews, see: a) E. Valeur, M. Bradley, *Chem. Soc. Rev.* **2009**, *38*, 606–631; b) V. R. Pattabiraman, J. W. Bode, *Nature* **2011**, *480*, 471–479; c) R. M. de Figueiredo, J.-S. Suppo, J.-M. Campagne, *Chem. Rev.* **2016**, *116*, 12029–12122.
- [5] For selected reviews, see: a) K. Pedrood, S. Bahadorikhalili, V. Lotfi, B. Larijani, M. Mahdavi, *Mol. Diversity* **2022**, *26*, 1311–1344; b) M. T. Sabatini, L. T. Boulton, H. F. Sneddon, T. D. Sheppard, *Nat. Catal.* **2019**, *2*, 10–17; c) E. Massolo, M. Pirola, M. Benaglia, *Eur. J. Org. Chem.* **2020**, 4641–4651; d) M. Todorovic, D. M. Perrin, *Pept. Sci.* **2020**, *112*, e24210.
- [6] J. Magano, *Org. Process Res. Dev.* **2022**, *26*, 1562–1689.
- [7] For selected reviews, see: a) K. L. Skubi, T. R. Blum, T. P. Yoon, *Chem. Rev.* **2016**, *116*, 10035–10074; b) N. A. Romero, D. A. Nicewicz, *Chem. Rev.* **2016**, *116*, 10075–10166; c) D. Cambié, C. Bottecchia, N. J. W. Straathof, V. Hessel, T. Noël, *Chem. Rev.* **2016**, *116*, 10276–10341; d) I. K. Sideri, E. Voutyritsa, C. G. Kokotos, *Org. Biomol. Chem.* **2018**, *16*, 4596–4614; e) M. Silvi, P. Melchiorre, *Nature* **2018**, *554*, 41–49; f) M. A. Theodoropoulou, N. F. Nikitas, C. G. Kokotos, *Beilstein J. Org. Chem.* **2020**, *16*, 833–857; g) S. Reischauer, B. Pieber, *iScience* **2021**, *24*, 102209; h) N. F. Nikitas, P. L. Gkizis, C. G. Kokotos, *Org. Biomol. Chem.* **2021**, *19*, 5237–5253; i) L. Capaldo, D. Ravelli, M. Fagnoni, *Chem. Rev.* **2022**, *122*, 1875–1924; j) E. Skolia, O. G. Mountanea, C. G. Kokotos, *Trends Chem.* **2023**, *5*, 116–120.
- [8] For a recent review, see: B. Lu, W.-J. Xiao, J.-R. Chen, *Molecules* **2022**, *27*, 517–558.
- [9] a) H. Liu, L. Zhao, Y. Yuan, Z. Xu, K. Chen, S. Qiu, H. Tan, *ACS Catal.* **2016**, *6*, 1732–1736; b) W. Song, K. Dong, M. Li, *Org. Lett.* **2020**, *22*, 371–375.
- [10] a) I. Cohen, A. K. Mishra, G. Parvari, R. Edrei, M. Dantus, Y. Eichen, A. M. Szpilman, *Chem. Commun.* **2017**, *53*, 10128–10131; b) A. K. Mishra, G. Parvari, S. K. Santra, A. Bazylevich, O. Dorfman, J. Rahamim, Y. Eichen, A. M. Szpilman, *Angew. Chem. Int. Ed.* **2021**, *60*, 12406–12412; *Angew. Chem.* **2021**, *133*, 12514–12520.
- [11] Y.-Q. Miao, J.-X. Kang, Y.-N. Ma, X. Chen, *Green Chem.* **2021**, *23*, 3595–3599.
- [12] J. Su, J.-N. Mo, X. Chen, A. Umanson, Z. Zhang, K. N. Houk, J. Zhao, *Angew. Chem. Int. Ed.* **2022**, *61*, e202112668.
- [13] a) E. Voutyritsa, C. G. Kokotos, *Angew. Chem. Int. Ed.* **2020**, *59*, 1735–1741; *Angew. Chem.* **2020**, *132*, 1752–1758; b) C. S. Batsika, C. Mantzourani, D. Gkikas, M. G. Kokotou, O. G. Mountanea, C. G. Kokotos, P. K. Politis, G. Kokotos, *J. Med. Chem.* **2021**, *64*, 5654–5666; c) E. Skolia, P. L. Gkizis, N. F. Nikitas, C. G. Kokotos, *Green Chem.* **2022**, *24*, 4108–4118; d) C. S. Batsika, C. Koutsilieris, G. S. Koutoulougenis, M. G. Kokotou, C. G. Kokotos, G. Kokotos, *Green Chem.* **2022**, *24*, 6224–6231; e) N. Spiliopoulou, P. L. Gkizis, I. Triandafillidi, N. F. Nikitas, C. S. Batsika, A. Bisticha, C. G. Kokotos, *Chem. Eur. J.* **2022**, *28*, e202200023.
- [14] a) G. N. Papadopoulos, C. G. Kokotos *J. Org. Chem.* **2016**, *81*, 7023–7028; b) N. F. Nikitas, M. K. Apostolopoulou, E. Skolia, A. Tsoukaki, C. G. Kokotos *Chem. Eur. J.* **2021**, *27*, 7915–7922.
- [15] a) R. S. Mulliken *J. Phys. Chem.* **1952**, *56*, 801–822. For selected reviews, see: b) T. M. Beale, M. G. Chudzinski, M. G. Sarwar, M. S. Taylor, *Chem. Soc. Rev.* **2013**, *42*, 1667–1680; c) G. Cavallo, P. Metrangolo, R. Milani, T. Pilati, A. Priimagi, G. Resnati, G. Terraneo, *Chem. Rev.* **2016**, *116*, 2478–2601.
- [16] For selected reviews, see: a) D. Bulfield, S. M. Huber, *Chem. Eur. J.* **2016**, *22*, 14434–14450; b) G. E. M. Crisenza, D. Mazzarella, P. Melchiorre, *J. Am. Chem. Soc.* **2020**, *142*, 5461–5476; For selected contributions, see: c) E. Arceo, I. D. Jurberg, A. Álvarez-Fernández, P. Melchiorre, *Nat. Chem.* **2013**, *5*, 750–756; d) Y.-Y. Liu, X.-Y. Yu, J.-R. Chen, M.-M. Qiao, X. Qi, D.-Q. Shi, W.-J. Xiao, *Angew. Chem. Int. Ed.* **2017**, *56*, 9527–9531; *Angew. Chem.* **2017**, *129*, 9655–9659; e) J. Börgel, L. Tanwar, F. Berger, T. Ritter, *J. Am. Chem. Soc.* **2018**, *140*, 16026–16031; f) S. Xie, D. Li, H. Huang, F. Zhang, Y. Chen, *J. Am. Chem. Soc.* **2019**, *141*, 16237–16242; g) L. M. Kammer, S. O. Badir, R.-M. Hu, G. A. Molander, *Chem. Sci.* **2021**, *12*, 5450–5457.
- [17] For detailed results and mechanistic studies, see Supporting Information.
- [18] T. A. Bramlett, A. J. Matzger, *Chem. Eur. J.* **2021**, *27*, 15472–15478.
- [19] J.-D. Chai, M. Head-Gordon, *Phys. Chem. Chem. Phys.* **2008**, *10*, 6615–6620.
- [20] F. Weigend, R. Ahlrichs, *Phys. Chem. Chem. Phys.* **2005**, *7*, 3297–3305.
- [21] C. E. Tzeliou, D. Tzeli, *J. Chem. Inf. Model.* **2022**, *62*, 6436–6448.
- [22] M. Carocho, P. Morales, I. C. F. R. Ferreira, *Food Chem. Toxicol.* **2017**, *107*, 302–317.
- [23] E. Berardesca, M. Iorizzo, E. Abril, G. Guglielmini, M. Caserini, R. Palmieri, G. E. Piérard, *J. Cosmet. Dermatol.* **2012**, *11*, 37–41.
- [24] a) M. Cycoń, M. Wojcik, S. Borymski, Z. Piotrowska-Seget, *Appl. Soil Ecol.* **2013**, *66*, 8–18; b) Y. Qi, D. Liu, W. Zhao, C. Liu, Z. Zhou, P. Wang, *Pestic. Biochem. Physiol.* **2015**, *125*, 38–44.
- [25] H. Zhu, B. Hu, H. Hua, C. Liu, Y. Cheng, Y. Guo, W. Yao, H. Qian, *Food Res. Int.* **2020**, *138*, 109819.
- [26] S. H. Burstein, *Mol. Pharmacol.* **2018**, *93*, 228–238.
- [27] For selected reviews and papers, see: a) L. Wang, W. Lv, X. Sun, F. Zheng, T. Xu, X. Liu, H. Li, X. Lu, Xi. Peng, C. Hu, G. Xu, *Anal. Chem.* **2021**, *93*, 10528–10537; b) I. Perkons, J. Rusko, D. Zacs, V. Bartkevics, *Sci. Total Environ.* **2021**, *755*, 142688; c) M. G. Kokotou, *Curr. Pharm. Anal.* **2020**, *16*, 513–519; d) M. G. M. de Sain-van der Velden, M. van der Ham, J. Gerrits, H. C. M. T. Prinsen, M. Willemsen, M. L. Pras-Raves, J. J. Jans, N. M. Verhoeven-Duijff, *Anal. Chim. Acta* **2017**, *979*, 45–50.
- [28] I. Triandafillidi, M. G. Kokotou, D. Lotter, C. Sparr, C. G. Kokotos, *Chem. Sci.* **2021**, *12*, 10191–10196.
- [29] M. Bodanszky, in *Principles of Peptide Synthesis*, Springer-Verlag, Berlin, Germany **1984**.
- [30] a) I. Shiina, H. Ushiyama, Y.-K. Yamada, Y.-I. Kawakita, K. Nakata, *Chem. Asian J.* **2008**, *3*, 454–461; b) K. Ishihara, Y. Lu, *Chem. Sci.* **2016**, *7*, 1276–1280.
- [31] a) M. Bodanszky, in *Principles of Peptide Synthesis*, Springer-Verlag, Berlin, Germany **1984**, Ch. 2; b) J. H. Jones, in *The Peptides*, Vol. 1 (Eds: E. Gross, J. Meienhofer), Academic Press, New York **1979**, Ch. 2.

Manuscript received: February 20, 2023

Accepted manuscript online: April 4, 2023

Version of record online: May 3, 2023